

A novel camera type for very high energy gamma-ray astronomy based on Geiger-mode avalanche photodiodes*

H. Anderhub,¹ M. Backes,² A. Biland,¹ A. Boller,¹ I. Braun,¹ T. Bretz,³ S. Commichau,¹
V. Commichau,¹ D. Dorner,^{1,4} A. Gendotti,¹ O. Grimm,¹ H. von Gunten,¹ D. Hildebrand,¹
U. Horisberger,¹ T. Krähenbühl,¹ D. Kranich,¹ E. Lorenz,^{1,5} W. Lustermann,¹
K. Mannheim,³ D. Neise,² F. Pauss,¹ D. Renker,⁶ W. Rhode,² M. Rissi,¹ U. Röser,¹
S. Rollke,² L. S. Stark,¹ J.-P. Stucki,¹ G. Viertel,¹ P. Vogler,¹ and Q. Weitzel^{1,†}

¹*Institute for Particle Physics, ETH Zurich,
Schafmattstr. 20, 8093 Zurich, Switzerland*

²*TU Dortmund University,
Otto-Hahn-Str. 4, 44227 Dortmund, Germany*

³*University of Würzburg,
Am Hubland, 97074 Würzburg, Germany*

⁴*ISDC Data Center for Astrophysics, University of Geneva,
Chemin d'Ecogia 16, 1290 Versoix, Switzerland*

⁵*Max Planck Institute for Physics,
Föhringer Ring 6, 80805 Munich, Germany*

⁶*Paul Scherrer Institute,
5232 Villigen PSI, Switzerland*

Geiger-mode avalanche photodiodes (G-APD) are promising new sensors for light detection in atmospheric Cherenkov telescopes. In this paper, the design and commissioning of a 36-pixel G-APD prototype camera is presented. The data acquisition is based on the Domino Ring Sampling (DRS2) chip. A sub-nanosecond time resolution has been achieved. Cosmic-ray induced air showers have been recorded using an imaging mirror setup, in a self-triggered mode. This is the first time that such measurements have been carried out with a complete G-APD camera.

*This is an author-created, un-copyedited version of an article published in Journal of Instrumentation. IOP Publishing Ltd is not responsible for any errors or omissions in this version of the manuscript or any version derived from it. The definitive publisher authenticated version is available online at <http://www.iop.org/EJ/abstract/1748-0221/4/10/P10010>.

†Corresponding author; Electronic address: qweitzel@phys.ethz.ch

I. INTRODUCTION

Imaging atmospheric Cherenkov telescopes (IACT) have been very successful in detecting very high energy ($\sim 0.1\text{--}30\text{ TeV}$) γ -rays from cosmic sources [1]. The key component is a pixelated camera which has to resolve flashes of Cherenkov light from air showers (duration 1–5 ns for γ -induced air showers, main wavelength range 300–650 nm). High-sensitivity photo-sensors are needed, even using light-collecting optics, since e. g. a 1 TeV primary photon hitting the atmosphere only results in about one hundred Cherenkov photons per square meter. Until now, matrices of photomultiplier tubes (PMT) have always been employed for this task. This is a well-known technology which, however, comes with some intrinsic disadvantages for telescope applications. PMTs are rather heavy and bulky, but at the same time fragile. They require high voltages of several 100 V or even kV and are damaged when exposed to sunlight. Typical PMTs furthermore have photon detection efficiencies (PDE) of only 20–30%.

Since a few years, a new type of semiconductor light-sensor is being developed, the so-called Geiger-mode avalanche photodiode (G-APD¹) [2]. These light-weight devices are built up from multiple APD cells operated in Geiger-mode. All the cells are connected in parallel and the overall signal is the sum of all simultaneously fired cells. They need bias voltages of 50–100 V, usually 1–5 V above the breakdown voltage. A high gain similar to PMTs is reached ($10^5\text{--}10^6$) and, potentially, higher PDEs of up to 50%. The market for G-APDs is continuously growing, and several manufacturers are working on their improvement. For an IACT application under realistic ambient conditions, several technical challenges have to be met. This mostly concerns the necessity to compensate for gain variations due to changes in temperature or night-sky background light (NSB). While the former is an intrinsic feature of G-APDs, the latter is a general problem and applies to other photo-sensors as well. An advantage of G-APDs is that they can be operated at NSB rates up to several GHz per sensor, thus allowing measurements under twilight and moonlight conditions.

First tests to detect Cherenkov light with small G-APD arrays have been performed in the past [3]. In order to develop a complete G-APD camera and find solutions for the technical challenges, the FACT project (First G-APD Camera Test) [4] has been launched. The prototype presented in this paper marks the first step towards a large camera with a field of view of about 5° ($0.1\text{--}0.2^\circ$ per pixel). This device is foreseen for the DWARF telescope (Dedicated multi-Wavelength AGN Research Facility) [5] which will perform monitoring of strong and varying γ -ray sources.

II. CAMERA LAYOUT AND FRONT-END ELECTRONICS

The prototype module comprises 144 G-APDs of type Hamamatsu MPPC S10362-33-50C [6]. Each has a sensitive area of $3\text{ mm} \times 3\text{ mm}$, covered by 3600 cells of $50\text{ }\mu\text{m} \times 50\text{ }\mu\text{m}$ size. The operating bias voltage ranges from 71.15 V to 71.55 V for the 144 sensors (at 25°C), corresponding to a gain of $7.5 \cdot 10^5$. The dark count rate is below 5 MHz. A non-imaging light collector is placed on top of each G-APD to compensate for dead spaces due to the diode-chip packaging (see figure 1, top part). Open aluminum cones with an affixed reflecting foil (ESR VikuitiTM by 3M) and a quadratic base are in use (bot-

¹ Also referred to as silicon photomultiplier (SiPM) or multi-pixel photon counter (MPPC).

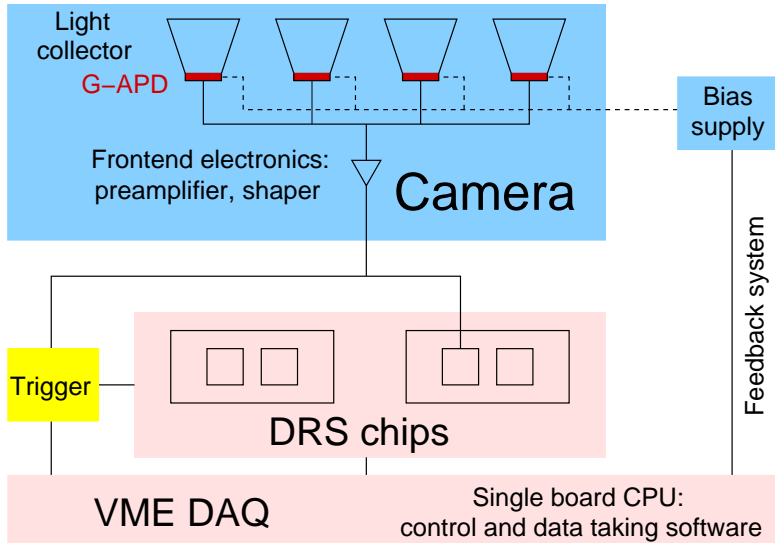


FIG. 1: Schematic overview of the G-APD camera layout (upper part) and the DAQ system (lower part); signal flow of one pixel shown. The camera is mounted inside a water-tight box, while the DAQ and trigger components are located in a counting room.

tom side: $2.8 \text{ mm} \times 2.8 \text{ mm}$, top side: $7.2 \text{ mm} \times 7.2 \text{ mm}$, height: 17.5 mm , effective solid angle: 0.55 sr). With such collectors, the NSB rate during the darkest nights at e.g. the Observatorio Roque de los Muchachos, La Palma, is $\sim 10 \text{ MHz}$ per sensor [7].

The signals from four G-APDs are summed up in front-end electronics boards (FEB) [8], resulting in 36 quadratic pixels of $14.4 \text{ mm} \times 14.4 \text{ mm}$ size. These boards also perform a signal shaping and amplification on the analog level (4 mV voltage output per μA current input, pulse decay times $< 10 \text{ ns}$). Each FEB comprises twelve channels, with a power consumption of 150 mW per channel. Figure 2 (left) shows a photograph of the camera module during assembly, including the FEBs. Also 16 of the 144 G-APDs are visible, and a block of four light collectors which are usually mounted on top of the sensors. Such a block corresponds to one pixel (readout channel).

In order to keep the gain of the G-APDs stable in case of changes of the ambient temperature and NSB conditions², a bias voltage feedback system has been foreseen. A calibration signal from a pulsed and temperature-stabilized light emitting diode can be monitored continuously and, if a change in amplitude is detected on a certain channel, the voltage of the corresponding pixel is modified to readjust the amplitude. Special power supply modules have been developed for this task [9], which can communicate with the camera control software (see also section III) via an USB interface and allow the bias voltage of each pixel to be regulated individually³. In addition, a water cooling system has been installed. An external cooling unit provides water of an adjustable temperature, which is pumped through copper tubes soldered onto a copper plate. The G-APDs are coupled to this plate by a thermally

² The NSB light produces a permanent current in a serial resistor of the readout electronics and thereby reduces the effective bias voltage, which is supplied through the FEBs.

³ Since four G-APDs are combined in one pixel, they have been selected such that their nominal operating voltages are within $\pm 10 \text{ mV}$. This translates into gain variations of a few percent [6].

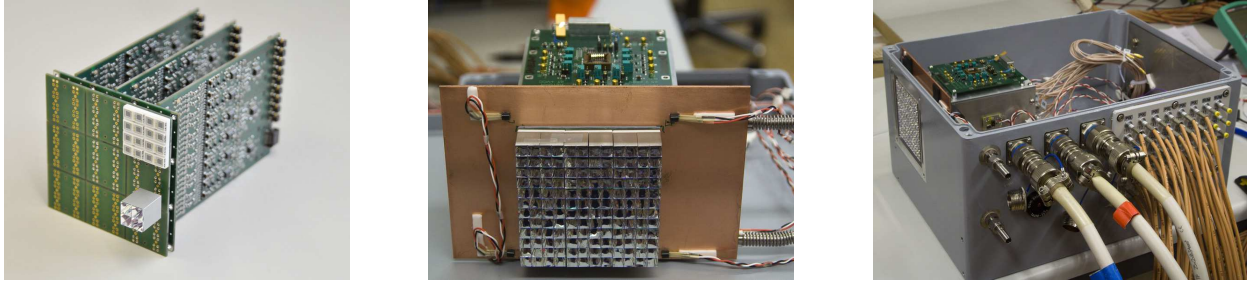


FIG. 2: Photographs taken during the camera assembly. Left: carrier PCB with 16 G-APDs ($\hat{=}$ 4 pixel) attached to the front, and the three front-end electronics boards attached to the back; a block of four light collectors ($\hat{=}$ 1 pixel) is mounted separately for demonstration purposes. Middle: fully assembled module including cooling plate. Right: integration into water-tight box; signal and voltage supply cables attached.

conductive but electrically insulating filling material. Several temperature sensors and one humidity sensor are used to monitor the conditions inside the box and on the cooling plate, as can be seen from figure 2 (middle). The cooling system is not obligatory to operate the sensors, but can be used optionally. The whole camera module is mounted inside a water-tight box (see figure 2, right), which has a protection window, a separate shutter (not shown in the photograph) and connectors for the signal and voltage supply cables.

III. TRIGGER AND DATA ACQUISITION SYSTEM

The analog signals are transferred from the camera box to the counting room by means of 20 m long coaxial cables. They are fed into linear fan-out modules (NIM standard) [10]. One module comprises twelve sub-units, each with one input channel and two normal and one inverted output channels. One of the (positive) outputs is connected to the data acquisition (DAQ) system, while the inverted (negative) signal is used for triggering purposes (see figure 1). The trigger logic consists of a CAEN V812 VME board where a majority coincidence of the innermost 16 pixels is formed. Individual trigger thresholds can be set via the VME bus.

The DAQ itself is based on the DRS2 (Domino Ring Sampling) chip [11] containing ten analog pipelines of 1024 capacitive cells. Signal sampling is performed with a frequency of 0.5–4.5 GHz, generated on-chip by a series of inverters. Such high sampling frequencies are desired for an IACT, since excellent timing significantly improves the reconstruction of the properties of the primary particle [12]. Each pipeline is read out at 40 MHz and externally digitized by a multiplexed 12 bit flash ADC (analog-to-digital converter). The DRS2 chips are mounted on mezzanine cards, which are hosted by VME boards (two chips per card and two cards per VME board). In this design, eight channels of each chip are available for external signals (see also [11]). A single-board computer is used as VME controller, with an attached hard disk for data storage. The DAQ and bias voltage control software are also running on this computer. For a trigger rate of 10 Hz, typical data rates are of the order of 1 MByte/s.

Sampling the signal with the ring sampler at frequencies in the GHz range allows a precise photon arrival time measurement, provided the so-called fixed-pattern aperture jitter of the

DRS2 chip is corrected. This relatively large, but systematic and gradual spread in its bin widths results from the manufacturing process. As the occurrence of a trigger is random with respect to the physical pipeline, the time measured between the trigger and the signal, being the sum of the widths of the involved bins, is also randomized to some degree. At 2 GHz sampling, this jitter can amount to about 5 ns and can have a complicated distribution, depending on the distance between trigger and signal. It can be corrected by calibrating with a high-frequency signal from a precision generator. The procedure involves measuring the period of this signal with the DRS2, and stretching or shrinking of the bin widths within that particular period to match the generator output. As the revolution frequency of the domino wave is phase locked to a stable oscillator, the revolution time (the sum over all 1024 individual bin widths) itself is fixed. Therefore, the inverse correction is applied to all bins outside the current period. Doing this for all periods of a sampled waveform and iteratively for many waveforms with random phase relative to the domino wave converges towards the required correction values. The effectiveness of the jitter correction is shown in figure 3 (left). The histograms show the time distributions of the rising edge of a pulse relative to the trigger signal with and without the correction at 2 GHz sampling frequency. Both the (square) test-pulse and the trigger were derived from a single output of a pulse generator. The correction values were determined in this case using a 200 MHz rectangular signal. After applying them, the pulse time distribution has a width of 390 ps root-mean-square.

IV. MEASUREMENT SETUP AND DATA TAKING PARAMETERS

In figure 3 (right) the experimental setup used for the detection of cosmic air showers is shown. The camera was mounted in the focus of a zenith-pointing spherical mirror (90 cm diameter). The focal length of the mirror was 80 cm which, taking into account the pixel dimensions, translates into a field of view of 1.0° per pixel. The measurements were performed during the night of July 2, 2009, near the city center of Zurich. Thus the NSB from surrounding buildings and also from partial moonlight was rather high. It was determined with an external sky quality meter (Unihedron) to be 300 MHz per G-APD (1.2 GHz per pixel). During the measurements, which took about an hour, the outdoor temperature was around 22°C . The G-APD plane was cooled to 18°C and the bias voltage for all pixels set to the nominal values for this temperature (~ 400 mV lower than for operation at 25°C). Under these stable conditions, no bias voltage feedback had to be used.

A sampling frequency of 2 GHz was set for the DRS2 chips. The trigger threshold was adjusted for each of the innermost 16 pixels, such that single pixel trigger rates of 1–3 kHz were obtained for an opened camera shutter. This was achieved by applying discriminator thresholds of 40 ± 4 mV to the analog signals⁴. A majority coincidence of four channels above threshold within a time window of 20 ns was furthermore required. Under these circumstances, the DAQ system recorded data with an average trigger rate of 0.02 Hz (also including noise triggers). The latency of the whole system was about 350 ns.

⁴ The thresholds had to be exceeded for at least 4 ns to fulfill the trigger requirement. A laboratory calibration, though without NSB light, showed that the analog readout features 7 mV signal amplitude per fired G-APD cell (approximately equivalent to the number of incoming photons per pixel multiplied with the PDE of the G-APDs).

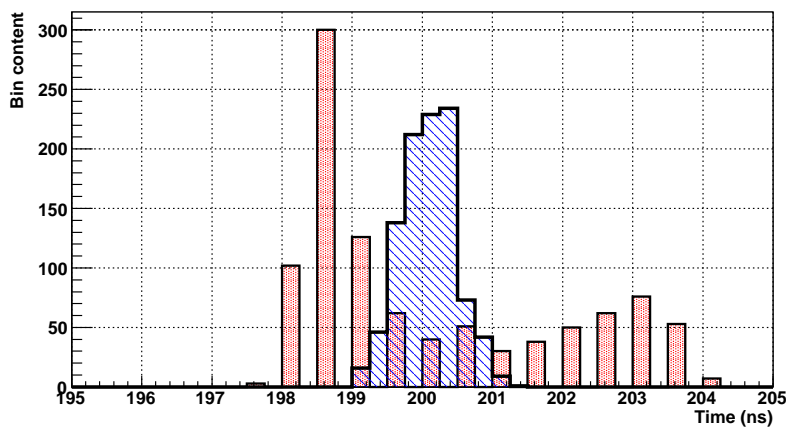


FIG. 3: Left: time distribution of square pulses sampled at 2 GHz with the DRS2 chip without (red filled histogram) and with jitter correction (blue shaded). The root-mean-square of the latter is 390 ns. Right: photograph of the experimental setup to record cosmic-ray induced air showers (see also text).

V. RESULTS AND DISCUSSION

For the offline analysis, events corresponding to Cherenkov light flashes have been filtered out from the recorded data. Several neighboring channels containing a clear signal, at the time position expected from the trigger latency, have been required. This is demonstrated in figure 4, which presents the raw data for a certain pixel (event #16 of run #207). The large plot shows the full DRS2 pipeline with a Cherenkov-light signal at about 160 ns, while the inset presents a zoom to the data between 0 and 150 ns. In the latter, the fluctuating signals from NSB photons are visible, which are very frequent and therefore pile up. The red line indicates the trigger threshold⁵. From the data analysis it has been estimated that the trigger rate for air shower events was about 0.01 Hz.

In figure 5 (left) the intensity distribution for the whole event introduced above is plotted. The maximum sample amplitude is shown on each of the 36 pixels, searched for within a time window of 100 ns around the expected signal position. Each amplitude has been corrected for the DRS2 baseline, evaluated event-by-event from the data samples recorded before the signal arrival (see figure 4). On the right side of figure 5, the jitter corrected (cf. section III) arrival time of the signals is presented⁶. Only pixels with a signal amplitude above 60 mV have been used for the timing calculation, the others are displayed in white color. A clear shower development is apparent for this event, starting in the top left corner of the display and extending to the bottom right corner within almost 20 ns. Figure 6 shows an event with a less extended time distribution (event #14 of run #206). Especially the core pixels with the largest amplitudes are within a few ns. The two outer pixels with a time offset of 3–4 ns compared to the core pixels are likely due to a sub-shower.

⁵ Translated to the digitized sample amplitudes. Please note that the signal is attenuated in front of the DRS2 chip to match its dynamic range.

⁶ Defined as the time of the last sample where the signal is below 50% of its amplitude (no interpolation).

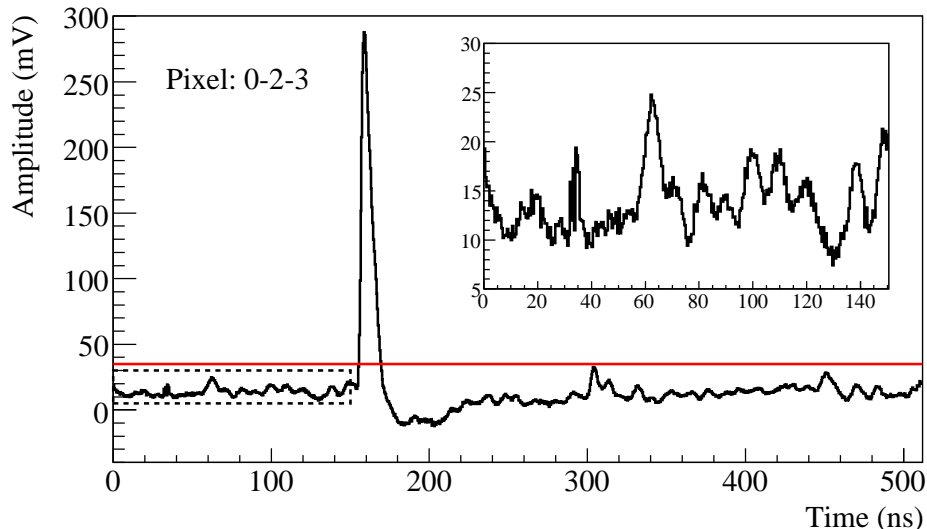


FIG. 4: Raw data of one pixel recorded with a sampling frequency of 2 GHz; full DRS2 pipeline shown. A Cherenkov-light signal can be seen at about 160 ns. The red solid line indicates the trigger threshold. The inset shows a zoom to the data from 0–150 ns as marked by the dashed-line box.

Taking into account that the camera covers a field of view of 6° in both dimensions (see also section IV), such events certainly come from air showers induced by very high energetic cosmic-ray particles. Dedicated simulations have been carried out⁷, concluding that the experimental setup described in this paper has an energy threshold of several TeV. Primary protons with off-axis angles up to 5° have been simulated⁸, and photon arrival time distributions consistent with the event presented in figure 6 have been observed. The event shown in figure 5 most probably corresponds to a primary particle with an off-axis angle of 10° or larger. Because of the comparatively long trigger coincidence window, it was possible to trigger such events.

VI. CONCLUSION

A 36-pixel prototype G-APD camera for Cherenkov astronomy has successfully been constructed and commissioned. A DAQ system based on the DRS2 chip has been set up. In a self-triggered mode, images of air showers induced by cosmic rays have been recorded. For the first time, this has been achieved with a complete G-APD camera. Stable operation at room temperature and under high NSB light conditions is possible. In summary, these photo-sensors have proven to fulfill the requirements of IACT applications, with the potential to replace or complement PMTs for future projects like the planned Cherenkov Telescope Array (CTA) [15].

⁷ The air shower simulation using CORSIKA [13], the detector simulation and data analysis using the MARS package (CheObs edition) [14].

⁸ Protons compose the largest fraction of the cosmic rays. Since in this case the mirror axis points up vertically to the sky, the off-axis angle coincides with the zenith angle.

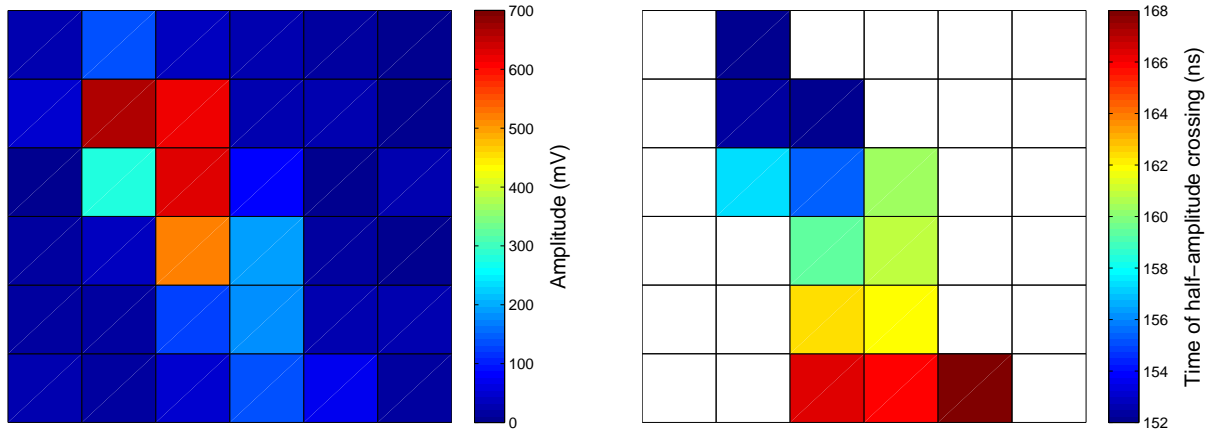


FIG. 5: Air shower image recorded with the G-APD camera (event #16 of run #207); the signal shown in figure 4 belongs to the pixel in the second column from the left, third row from the top. Left: intensity distribution over the 6 pixels \times 6 pixels. Right: corresponding signal arrival time distribution (see text).

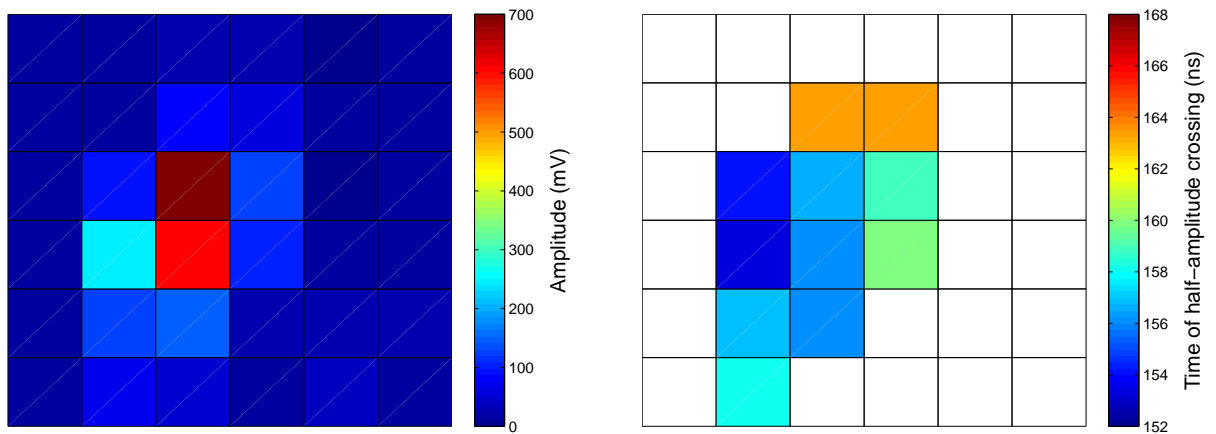


FIG. 6: Further air shower image recorded with the G-APD camera (event #14 of run #206). Left: intensity distribution over the 6 pixels \times 6 pixels. Right: corresponding signal arrival time distribution (see text). The color scales are the same as in figure 5.

Acknowledgments

This work is supported by ETH research grants 0-43391-08 and 0-20486-08.

-
- [1] F. Aharonian et al., *High energy astrophysics with ground-based gamma ray detectors*, Rep. Prog. Phys. **71** (2008) 096901.
- [2] D. Renker and E. Lorenz, *Advances in solid state photon detectors*, JINST **4** (2009) P04004.
- [3] A. Biland et al., *First detection of air shower Cherenkov light by Geigermode-avalanche photodiodes*, Nucl. Instrum. Meth. **A595** (2008) 165.
- [4] I. Braun et al., *First avalanche-photodiode camera test (FACT): a novel camera using G-APDs for the observation of very high-energy gamma-rays with Cherenkov telescopes*, in proceedings of *5th International Conference on New Developments in Photodetection*, June, 15–20, 2008, Aix-les-Bains, France, in press at Nucl. Instrum. Meth. **A**.
- [5] T. Bretz et al., *Long-term monitoring of bright blazars with a dedicated Cherenkov telescope*, in proceedings of *4th International Meeting on High Energy Gamma-Ray Astronomy*, July, 7–11, 2008, Heidelberg, Germany, AIP Conf. Proc. **1085** (2008) 850.
- [6] Hamamatsu Photonics, Shizuoka, Japan, <http://www.hamamatsu.com>, *MPPC data sheet*, (2008).
- [7] R. Mirzoyan and E. Lorenz, *Measurement of the night sky light background at La Palma*, Max Planck Institute for Physics, Munich, Report MPI-PhE **94-35** (1994).
- [8] L. S. Stark and U. Röser, *Test of the 16-fold G-APD preamplifier PAG-20 including strong NSB*, ETH Zurich, Internal Report (2008).
- [9] V. Commichau et al., *Multi-channel G-APD bias voltage supply*, ETH Zurich, Internal Report (2008).
- [10] M. Morf and U. Röser, *Verteilerschaltung FAN-OUT_6*, ETH Zurich, Internal Report (2009).
- [11] S. Ritt, *The DRS2 chip: a 4.5 GHz waveform digitizing chip for the MEG experiment*, in proceedings of *IEEE Nuclear Science Symposium*, October, 16–22, 2004, Rome, Italy, Conf. Rec. **2** (2004) 974.
- [12] E. Aliu et al., *Improving the performance of the single-dish Cherenkov telescope MAGIC through the use of signal timing*, Astropart. Phys. **30** (2009) 293.
- [13] D. Heck et al., *CORSIKA: a Monte Carlo code to simulate extensive air showers*, Forschungszentrum Karlsruhe, Report FZKA **6019** (1998).
- [14] T. Bretz and D. Dorner, *MARS-CheObs goes Monte Carlo*, in proceedings of *31st International Cosmic Ray Conference*, July, 7–15, 2009, Lodz, Poland, to be published online at <http://icrc2009.uni.lodz.pl>.
- [15] CTA consortium, <http://www.cta-observatory.org>, *Conceptual design report* in preparation.